


Proceedings Article

Optimizing magnetic particle image resolution using superferromagnetic nanoparticles modified through post-synthesis oxidation

Jacob Bryan^{a,*}, Benjamin Fellows^{a,*}, K.L Barry Fung^a, Prashant Chandrasekharan ^a, Steven Conolly^{a,b}

^aDepartment of Bioengineering, UC Berkeley, Berkeley CA, USA

^bDepartment of Electrical Engineering and Computer Science, UC Berkeley, Berkeley CA, USA

*Corresponding author, email: jacobbryan1124@berkeley.edu; bdfello@berkeley.edu

© 2022 Jacob Bryan *et al.*; licensee Infinite Science Publishing GmbH

This is an Open Access article distributed under the terms of the Creative Commons Attribution License (<http://creativecommons.org/licenses/by/4.0>), which permits unrestricted use, distribution, and reproduction in any medium, provided the original work is properly cited.

Abstract

Magnetic Particle Imaging (MPI) is a novel tracer-based imaging modality that allows for exquisitely sensitive cell therapy tracking *in vivo*, cancer imaging, lung ventilation/perfusion imaging, and hemorrhage detection. MPI uses superparamagnetic iron oxide Particles (SPIOs) as tracers with linear contrast, zero tissue attenuation, and micromolar sensitivity, all with zero ionizing radiation and infinite reporter persistence. However, MPI's poor spatial resolution (roughly 1 mm in a 7T/m gradient) is holding back clinical translation. Using an arbitrary waveform relaxometer (AWR) which is similar to an MPS in that it is used to characterize the magnetics of the nanoparticles, our lab recently reported the use of superferromagnetic nanoparticles (SFMIOs) for MPI demonstrating a 10-fold improvement ($\approx 100\mu\text{m}$) in resolution compared to the approximately 1 mm for commercially available SPIOs. In the current work, we detail the production of SFMIOs for MPI using a modified extended LaMer synthesis. We implement a post-oxidation step to the process for repeated and reproducible production of high resolution SFMIO particles.

1. Introduction

The resolution in magnetic particle imaging (MPI) depends on the magnetic property of the superparamagnetic iron oxide (SPIOs) particles and the gradient strength of the scanner [1, 2]. The magnetic resolution of SPIO depends on the slope of the linear part of the Langevin function and by improving the magnetic property (dM/dH) one can improve the resolution of the images in MPI. The Langevin physics predicts a cubic improvement in the magnetic properties with increase in size of the particles, however, larger size particles are affected by relaxation delay causing blurring rather than improving MPI resolution [2, 3].

In a pioneering work from our lab, we reported the use of superferromagnetic nanoparticles with a near ideal dM/dH that shows almost a step like response with the applied field [4], improving MPI resolution by almost 10-fold compared to commercially available particles. Unlike superparamagnetic nanoparticles, superferromagnetic nanoparticles interact with each other's local magnetic fields and form chains. The dipole interaction and chaining of the strongly-interacting nanoparticles is believed to cause SFMIO behaviour. The extended La Mer's method of magnetic particle synthesis provides great control over particle size and thus their magnetic properties [5] for SFMIO synthesis. The thermal decomposition method of particle preparation uses metal-organic pre-

cursors that form crystalline nanoparticles under control conditions. However, in the process the crystalline iron oxide phase of nanoparticle is often surrounded by magnetically "dead layer" or contain partially oxidized core. Controlled oxidation of the dead layer and core has shown to both improve the crystalline phase of the particles as well as the magnetic properties of the particles [6–8]. In this work, we evaluate the effect of ripening and under varying oxidative conditions and their effect on MPI image resolution.

II. Methods and Materials

Iron oxide nanoparticles are synthesized in three steps and follows a procedure similar to that used in Vreeland et al [5]. First, to produce the base iron oleate precursor, we react iron (III) acetylacetonate (3.3g) with oleic acid (15ml) at 320°C for 30 minutes. The reaction is kept under a constant nitrogen gas. once synthesized, the precursor is used without purification. This preserves the iron stoichiometry within the oleate, as the added iron (III) acetylacetonate₃ is a crystalline solid, and is used to estimate iron concentration of the precursor.

Once the iron oleate precursor is made, it is diluted to to the chosen working concentration (0.223M) by using octadecene. The diluted precursor is added to a syringe and to be dripped into our reaction in a separate 3 neck, 150ml flask, 5.1 ml of octadecene is added and both the side necks are sealed using teflon septa. The precursor syringe with penetration needle is punctured into the Teflon septum of the reaction flask. An initial nitrogen purge is done at high flow (30s at > 1LPM), the flow is then reduced extensively to reduce solvent/surfactant loss at high temperatures. The reaction flask lowered into a solder bath at 290°C, and the precursor syringe is hooked into a syringe pump. An overhead stirrer is inserted into the middle neck and set to stir at 400rpm. Once the reaction is assembled, the temperature of the reaction bath is increased to 360°C. Once the temperature is stable, the iron oleate precursor is dripped in at a rate of 6mL/hour for 25 minutes.

After particle synthesis, we test various post-synthesis oxidation and annealing steps to optimize particle resolution as highlighted below. Particles are then suspended in hexane and washed via centrifuge. Magnetic properties were analyzed in our arbitrary waveform relaxometer (AWR) [9] at a frequency of 20 kHz and excitation amplitudes ranging from 2-24 mT. For further technical details on the AWR, please see the cited paper.

III. Experiments and Results

After iron oleate precursor is dripped into the reaction flask for 25 minutes, we tested to see the significance

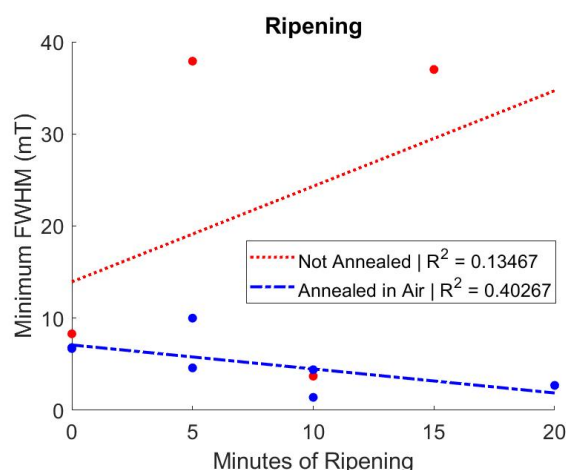


Figure 1: FWHM of the particle PSF with ripening times ranging from 0 to 20 minutes in nitrogen. Non-oxidized particles (red) were washed immediately after ripening. Oxidized particles (blue) were washed after annealing for 12 hours exposed to air.

of heating our particles in nitrogen for a variable period of time—effectively enforcing a ripening event [10]. Thereafter, if we left our particles to anneal in air for an extended period of time after ripening (over 12 hours), we saw a significant improvement and consistency in full width at half maximum (FWHM) resolution (see Figure ??). However, if we washed particles immediately without annealing, there was no significant improvement in SFMIO behavior despite the ripening step. Proving the importance of both ripening our particles at high temperatures and annealing our particles exposed to air post-synthesis.

To determine if an oxidation step during annealing was more important rather than simply annealing, synthesis procedures were compared after 10 minutes of ripening. We annealed freshly synthesized particles overnight in nitrogen gas versus particles annealed overnight exposed to air. The particles exposed to air produced our highest resolution particles as of yet, with a narrow point-spread-function (PSF) and a FWHM resolution of 0.8 mT (see Figure 2). On average, the particles annealed in air showed a 60% improvement in FWHM resolution and a 70% improvement in FWHM standard deviation relative to particles annealed under inert conditions of nitrogen (see Figure 3), which describes a dependency on oxidation after synthesis.

IV. Discussion

Oxidation of "magnetically dead layer" can generate pure phase wüstite and magnetite iron oxide nanoparticles [6, 8]. The pure crystalline phases of the particles greatly improve the magnetic properties and thus the MPI per-

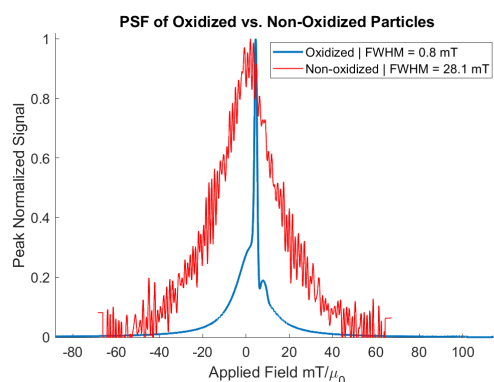


Figure 2: PSF of 0.8 mT resolution iron oxide nanoparticles annealed in air compared to particles annealed in nitrogen.

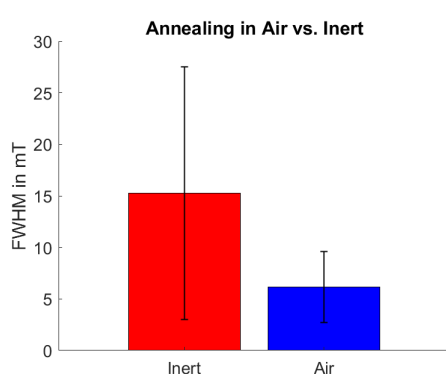


Figure 3: FWHM of particles' PSF left overnight in air compared to particles in nitrogen. Bars signify standard deviation.

formance. Annealing of SFMIO particles in air provided consistent and reproducible production of high resolution MPI particles (≤ 1.5 mT).

V. Conclusion

By elucidating the importance of the post-synthesis ripening and oxidation, we have greatly improved the FWHM of our particles' PSF and consistency of high resolution SFMIO particles, but further research is needed to allow for more consistent high-resolution particles. Currently, particles with a resolution of 1.5 mT or better are synthesized less than 10% of the time. This is a result of the many oxidation phases that iron oxide nanoparticles have. Further studies need to be conducted to characterize the synthesized SFMIO particles and also increase phase control by more precisely modulating oxidation by the addition of a heated oil bath and continuous monitoring of FWHM resolution over time.

Acknowledgments

We gratefully acknowledge support from NIH grants R01s EB019458, EB024578, EB029822 and R44: EB029877, UC TRDRP grant 26IP-0049, M. Cook Chair, Bakar Fellowship, the Siebel fellowship, the UC Discovery Award.

Author's statement

Conflict of interest: Prof. Conolly is a co-founder of a startup company, Magnetic Insights, Inc, that manufactures and sells preclinical MPI scanners.

References

- [1] P. Chandrasekharan, Z. W. Tay, X. Y. Zhou, E. Y. Yu, B. K. Fung, C. Colson, B. D. Fellows, Y. Lu, Q. Huynh, C. Saayujya, P. Keselman, D. Hensley, K. Lu, R. Orendorff, J. Konkle, E. U. Saritas, B. Zheng, P. Goodwill, and S. Conolly, Chapter 15 - magnetic particle imaging for vascular, cellular and molecular imaging, in *Molecular Imaging (Second Edition)*, B. D. Ross and S. S. Gambhir, Eds., Second Edition, Academic Press, 2021, 265–282, ISBN: 978-0-12-816386-3. doi:<https://doi.org/10.1016/B978-0-12-816386-3.00015-6>.
- [2] Z. W. Tay, D. W. Hensley, E. C. Vreeland, B. Zheng, and S. M. Conolly. The Relaxation Wall: Experimental Limits to Improving MPI Spatial Resolution by Increasing Nanoparticle Core size. *Biomed Phys Eng Express*, 3(3), 2017, doi:[10.1088/2057-1976/aa6ab6](https://doi.org/10.1088/2057-1976/aa6ab6).
- [3] Z. W. Tay, D. Hensley, J. Ma, P. Chandrasekharan, B. Zheng, P. Goodwill, and S. Conolly. Pulsed Excitation in Magnetic Particle Imaging. *IEEE Trans Med Imaging*, 38(10):2389–2399, 2019, doi:[10.1109/TMI.2019.2898202](https://doi.org/10.1109/TMI.2019.2898202).
- [4] Z. W. Tay, S. Savliwala, D. W. Hensley, K. B. Fung, C. Colson, B. D. Fellows, X. Zhou, Q. Huynh, Y. Lu, B. Zheng, P. Chandrasekharan, S. M. Rivera-Jimenez, C. M. Rinaldi-Ramos, and S. M. Conolly. Superferromagnetic nanoparticles enable order-of-magnitude resolution & sensitivity gain in magnetic particle imaging. *Small Methods*, 5(11):2100796, 2021, doi:<https://doi.org/10.1002/smt.202100796>.
- [5] E. C. Vreeland, J. Watt, G. B. Schober, B. G. Hance, M. J. Austin, A. D. Price, B. D. Fellows, T. C. Monson, N. S. Hudak, L. Maldonado-Camargo, A. C. Bohorquez, C. Rinaldi, and D. L. Huber. Enhanced nanoparticle size control by extending lamer's mechanism. *Chemistry of Materials*, 27(17):6059–6066, 2015, doi:[10.1021/acs.chemmater.5b02510](https://doi.org/10.1021/acs.chemmater.5b02510).
- [6] Z. Yan, S. FitzGerald, T. M. Crawford, and O. T. Mefford. Oxidation of wüstite rich iron oxide nanoparticles via post-synthesis annealing. *Journal of Magnetism and Magnetic Materials*, 539:168405, 2021, doi:<https://doi.org/10.1016/j.jmmm.2021.168405>.
- [7] M. Unni, A. M. Uhl, S. Savliwala, B. H. Savitzky, R. Dhavalikar, N. Garraud, D. P. Arnold, L. F. Kourkoutis, J. S. Andrew, and C. Rinaldi. Thermal decomposition synthesis of iron oxide nanoparticles with diminished magnetic dead layer by controlled addition of oxygen. *ACS Nano*, 11(2):2284–2303, 2017, PMID: 28178419. doi:[10.1021/acs.nano.7b00609](https://doi.org/10.1021/acs.nano.7b00609).
- [8] R. Hufschmid, H. Arami, R. M. Ferguson, M. Gonzales, E. Teeman, L. N. Brush, N. D. Browning, and K. M. Krishnan. Synthesis of phase-pure and monodisperse iron oxide nanoparticles by thermal decomposition. *Nanoscale*, 7:11142–11154, 25 2015, doi:[10.1039/C5NR01651G](https://doi.org/10.1039/C5NR01651G).
- [9] Z. W. Tay, Goodwill, D. Hensley, L. Taylor, B. Zheng, and S. Conolly. A High-Throughput, Arbitrary-Waveform, MPI Spectrometer and Relaxometer for Comprehensive Magnetic Particle Optimization and Characterization. *Nature Scientific Reports*, 34180(30), 2016, doi:[10.1038/srep34180](https://doi.org/10.1038/srep34180).

- [10] S. P. Utami, A. Fadli, E. O. Sari, and A. S. Addabsi. Crystal-growth kinetics of magnetite (Fe_3O_4) nanoparticles with ostwald ripening model approach. *IOP Conference Series: Materials Science and Engineering*, 345:012010, 2018, doi:[10.1088/1757-899x/345/1/012010](https://doi.org/10.1088/1757-899x/345/1/012010).